Monthly Notices
of the
ROYAL ASTRONOMICAL SOCIETY

Mon. Not. R. Astron. Soc. **404,** 1672–1678 (2010) doi:10.1111/j.1365-2966.2010.16408.x

Contamination on Lyman continuum emission at $z \gtrsim 3$: implication on the ionizing radiation evolution⋆

E. Vanzella,[1]† B. Siana,[2] S. Cristiani[1] and M. Nonino[1]

[1]*INAF – Osservatorio Astronomico di Trieste, Via G.B. Tiepolo 11, 40131 Trieste, Italy*
[2]*California Institute of Technology, MS 105-24, Pasadena, CA 91125, USA*

Accepted 2010 January 22. Received 2010 January 19; in original form 2009 November 17

ABSTRACT

We investigate the possibility of contamination by lower redshift interlopers in the measure of the ionizing radiation escaping from high-redshift galaxies. Taking advantage of the new ultradeep Very Large Telescope/Visible Multiobject Spectrograph U-band number counts in the Great Observatories Origins Deep Survey (GOODS)-South field, we calculate the expected probability of contamination by low-redshift interlopers as a function of the U magnitude and the image spatial resolution (point spread function). Assuming that ground-based imaging or spectroscopy cannot resolve objects lying within a 0.5-arcsec radius of each other, then each $z \gtrsim 3$ galaxy has a 2.1 and 3.2 per cent chance of foreground contamination, adopting surface density U-band number counts down to 27.5 and 28.5, respectively. Those probabilities increase to 8.5 and 12.6 per cent, assuming 1.0-arcsec radius. If applied to the estimates reported in the literature at redshift $\sim$3 for which a Lyman continuum has been observed directly, the probability that at least one-third of them are affected by foreground contamination is larger than 50 per cent. From a Monte Carlo simulation, we estimate the median integrated contribution of foreground sources to the Lyman continuum flux ($f900$). Current estimations from stacked data are $>2\sigma$ of the median integrated pollution by foreground sources. If the correction to the observed $f900$ flux is applied, the relative escape fraction decreases by a factor of $\sim$1.3 and 2, depending on the cases reported in literature. The spatial cross-correlation between the U-band ultradeep catalogue and a sample of galaxies at $z \gtrsim 3.4$ in the GOODS-South field produces a number of U-band detected systems fully consistent with the expected superposition statistics. Indeed, each of them shows the presence of at least one offset contaminant in the Advanced Camera for Surveys images. An exemplary case of a foreground contamination in the *Hubble Ultra Deep Field* at redshift 3.797 by a foreground blue compact source ($U = 28.63 \pm 0.2$) is reported; if observed with a low-resolution image (seeing larger than 0.5 arcsec) the polluting source would mimic an observed $(f1500/f900)_{\rm OBS} \sim 38$, erroneously ascribed to the source at higher redshift.

Key words: galaxies: evolution – galaxies: high-redshift – intergalactic medium – cosmology: observations – diffuse radiation.

1 INTRODUCTION

Ionizing radiation from star-forming galaxies is a plausible primary source of cosmic re-ionization. The amount, the evolution with redshift and its contribution to the cosmic re-ionization is still a matter of debate (e.g. Steidel, Pettini & Adelberger 2001; Giallongo et al. 2002; Shapley et al. 2006, hereafter S06; Siana et al. 2007, 2010; Faucher-Giguère et al. 2008; Iwata et al. 2009, hereafter I09).

Malkan, Webb & Konopacky (2003) and Siana et al. (2007, 2010) have stacked 10s of deep ultraviolet (UV) imaged galaxies at redshift $\sim$1 and no detection has been reported. Similarly, Cowie, Barger & Trouille (2009) have combined $\sim$600 galaxies observed with *Galaxy Evolution Explorer* (*GALEX*) at the same redshift, and also in this case the result was a non-detection. At higher redshift ($z > 3$), an escape of Lyman continuum photons (hereafter LyC) seems to be detected in $\sim$10 per cent of the galaxies (e.g. I09 and S06), suggesting a possible evolution of the escape fraction with redshift. It is still unclear which is the typical escape fraction to be expected from starburst galaxies at redshift $z \gtrsim 3$. While some results of

⋆Based on observations made at the European Southern Observatory (ESO), Paranal, Chile (ESO programme 170.A-0788. The Great Observatories Origins Deep Survey: ESO Public Observations of the *SIRTF* Legacy/*HST* Treasury/*Chandra Deep Field* South).

†E-mail: vanzella@oats.inaf.it

numerical simulations suggest low values (less than 10 per cent; e.g. Gnedin, Kravtsov & Chen 2008), others claim escape fraction as high as 80 per cent (e.g. Razoumov & Sommer-Larsen 2010; Yajima et al. 2009). The two possibilities imply two completely different scenarios: in the first case, high-redshift galaxies turn out to be inefficient in releasing ionizing radiation into the intergalactic medium; conversely in the second case, they may play a dominant role in this redshift regime.

As redshift increases, the probability of foreground contamination by blue galaxies that mimic the ionizing radiation also increases. Therefore, it is important to study the contaminated systems and try to quantify their occurrences. The recent ultradeep Very Large Telescope (VLT)/Visible Multiobject Spectrograph (VIMOS) *U*-band observations in the Great Observatories Origins Deep Survey (GOODS)-S field (Nonino et al. 2009) allow us to investigate this issue to unprecedented depth and to better calculate the probability of such contamination (a comparison between the observed superpositions in the GOODS-S area and those expected is also performed). Very deep exposures with exquisite spatial resolution, as the *Hubble Ultra Deep Field* (*HUDF*; Beckwith et al. 2006), make it possible to verify the results of such a calculation over limited areas of the sky. The work is structured as follows: in Section 2.1, the probability distributions of foreground superposition are calculated, and in Section 2.2 it is compared to the observed direct detections reported in literature. In Section 2.3, the Monte Carlo simulations are described to derive the integrated contribution of foreground sources. In Section 3, the *U*-band catalogue is cross-matched to the redshift ∼4 sample and checked for contamination. Section 3.1 discusses the case of an exemplary false LyC escape detection in the *HUDF*. Section 4 summarizes the results. The standard cosmology is adopted ($H_0 = 70\,\mathrm{km\,s^{-1}\,Mpc^{-1}}$, $\Omega_\mathrm{M} = 0.3$, $\Omega_\Lambda = 0.7$). If not specified, magnitudes are given in AB system.

2 LYMAN CONTINUUM ESCAPE RADIATION AT $z > 3$

2.1 The expected probability of foreground contamination

Taking advantage of the ultradeep VIMOS *U*-band imaging in the GOODS-S field (Nonino et al. 2009), that reaches magnitude 29.8 (28.5) at 1σ (3σ) within 1-arcsec aperture (radius), we determine the likelihood of foreground contamination of $z > 3$, as these galaxies must reside in the foreground and are emitting at wavelengths that mimic LyC of Lyman break galaxies (LBGs). Similar to the discussion in Siana et al. (2007), we assume that the spatial distribution of the foreground (*U*-detected) galaxies is uniform and uncorrelated with those at higher redshift. If we adopt the surface density of objects with $U(\mathrm{AB}) < 28.5$ (520200 deg^{-2}; see Table 1 and Nonino et al. 2009) and assume that ground-based imaging or spectroscopy cannot resolve objects which lie within a 0.5 (0.8) arcsec radius of each other, than we would expect that each $z \gtrsim 3$ galaxy has a $p \sim 3.2$ (8.1) per cent chance of foreground contamination. Fig. 1 summarizes the probabilities that a certain fraction (per cent) of the total sample N is contaminated by foreground sources, as a function of the seeing and *U*-band number counts.[1] It is evident that increasing the *U*-band magnitude limit of galaxy counts and the seeing value, the probability of foreground contamination increases. Depending on the seeing conditions and the *U*-band magnitude limit adopted, the fraction of the population contaminated by foreground sources ranges between 3 and 15 per cent, more severely if the faint fluxes are investigated (see Fig. 1). Currently, the direct LyC detections reported in literature regard fractions smaller than 15 per cent. It is worth noting that stacking of sources can also be affected by contamination, being a result of a sum that may include contaminated cases not detected individually (see Section 2.3). In the following sections, we consider the observed number counts down to *U*-mag 28.5 (3σ limit), beyond this limit a linear extrapolation is performed (see Section 2.3). In the next section, the derived probabilities are compared to the observations of direct LyC.

[1] The probability to observe K (or $\geq K$) contaminated sources in a sample of N ($> K$) high-z galaxies, given the probability p of the single case, is

$$f(K) = \binom{N}{K} p^K (1-p)^{N-K}; \qquad P(\geq K) = \sum_{i=k}^{N} f(i).$$

Table 1. Number counts derived from the ultradeep VLT/VIMOS catalogue down to $U \sim 30$ (1σ limit within 1-arcsec aperture radius; Nonino et al. 2009). Completeness correction has been roughly applied at magnitudes fainter than 28.5 ($\sim 3\sigma$ limit). The values in parenthesis have been calculated by extrapolating linearly the number counts up to *U*-mag 30.5 by fitting a straight line in the range *U*-mag 25–28 with a slope of 0.2 in the [log(N)] versus [*U*-mag] plane.

U-mag U_low–U_up	N (counts) (deg^{-2})	Cumul ($m < U_\mathrm{up}$) (deg^{-2})
22.0–22.5	1400 ± 40	1400
22.5–23.0	2200 ± 50	3600
23.0–23.5	4400 ± 70	8000
23.5–24.0	8300 ± 90	16 300
24.0–24.5	14 900 ± 120	31 200
24.5–25.0	23 800 ± 150	55 000
25.0–25.5	33 500 ± 180	88 500
25.5–26.0	45 600 ± 210	134 000
26.0–26.5	57 900 ± 240	191 900
26.5–27.0	72 300 ± 270	264 200
27.0–27.5	85 300 ± 270	349 500
27.5–28.0	90 200 ± 300	439 700
28.0–28.5	80 400 ± 280	520 200
28.5–29.0	54 900 ± 230 (177 800)	575 100 (698 000)
29.0–29.5	23 700 ± 150 (223 900)	598 800 (921 900)
29.5–30.0	4500 ± 70 (281 800)	603 300 (123 700)
30.0–30.5	(354 800)	603 300 (1558 500)

2.2 The current LyC detections

S06 reported on LyC detections: two out of 14 galaxies show a clear signal below 912 Å rest-frame in their deep spectra. In particular, SSA22a-C49 ($z = 3.115$) and SSA22a-D3 ($z = 3.067$) show a LyC flux of $f_{900} = (11.8 \pm 1.1) \times 10^{-31}\,\mathrm{erg\,s^{-1}\,cm^{-2}\,Hz^{-1}}$ [mag(AB) = 26.22] and $f_{900} = (6.9 \pm 1.0) \times 10^{-31}\,\mathrm{erg\,s^{-1}\,cm^{-2}\,Hz^{-1}}$ [mag(AB) = 26.80], respectively. Adopting the seeing value reported in S06, never worse than 1.0 arcsec and larger than 0.8 arcsec, and the number counts in the magnitude range $26 < U < 27$ (130200 deg^{-2}), the probabilities that at least one galaxy (out of 14) in the S06 study is subject to foreground contamination assuming seeing 0.8, 0.9 and 1.0 arcsec are 25, 30 and 36 per cent, respectively. There is a 3, 5 and 7 per cent chance that at least two detections are contaminated.

It is worth noting that in the case of spectroscopic observations, the slit width (1.2 arcsec in S06) and its orientation on the sky may influence the net contribution of a close ('sub-seeing') contaminant, since it may be partially included in the slit if there is a spatial

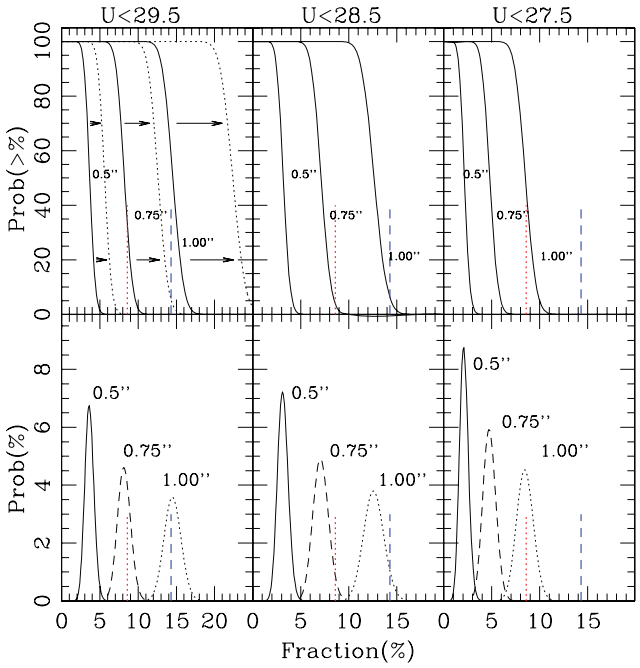

Figure 1. Probabilities (Prob, *y*-axis) that a fraction (per cent, *x*-axis) of an observed sample is contaminated by foreground sources. Calculations have been performed varying the single case probability, p, in turns related to the U-band number counts (from left- to right-hand panels) and seeing (different curves in each panel). Top panels: the cumulative probability distribution versus fractions (per cent) of the entire sample (N). It is the probability that at least a fraction K (per cent) of the N galaxies observed [$P(\geq K)$ with $N > K$] is contaminated by foreground sources. In the fainter limit case, U-mag $<$ 29.5 (left-hand panel), calculations have been performed with the observed number counts (solid lines) and those corrected by incompleteness in the range 28.5 $< U$-mag $<$ 29.5 (dotted lines, see text for details). The arrows show how the curves change from uncorrected to corrected. Bottom panels: the probability distributions that a fraction K(per cent) of the N galaxies observed [$P(K)$] are contaminated. Increasing the U-band surface density and the seeing, the probability of superposition increases. In all the panels, the two vertical dotted (red) and dashed (blue) lines mark the percentages of the direct LyC detections by I09 (17/198) and S06 (2/14), respectively.

offset. Therefore, the $f900$ flux due to offset foreground sources is decreased. In principle, there is also the additional possibility to identify the foreground source through its spectral features if the emission lines are present in the wavelength range and are intense enough to be detected.

I09 reported similar LyC detections in LBGs and Lyman alpha emitters (LAEs) at redshift 3.1 with dedicated narrow-band imaging (NB359). In particular, 17 (seven LBGs and 10 LAEs) sources out of 198 (73 LBGs and 125 LAEs) show a clear signal ($\gtrsim 3\sigma$). Looking at their fig. 4, the NB359 magnitude of the 17 cases is in the range 26–27.5, the surface density of U-band detected galaxies in this interval is 215 500 deg^{-2} (Nonino et al. 2009). Assuming, as in I09, that a foreground object within 1.0-arcsec radius cannot be distinguished in the image, each object has 5.2 per cent chance of contamination, corresponding to a 59 (46) per cent chance that at least (10/11) sources out of 198 are contaminated by foregrounds. If we adopt a U-mag range 26.5–27.5 as in I09, the U surface density becomes 157 600 deg^{-2}, corresponding to a 49 per cent of probability that at least eight objects out of 198 are contaminated. Furthermore, I09 noted that shapes and positions of the emitting regions in the sub-sample of LBGs are different from those in the R band, reporting an average offset of 0.97 arcsec. Since spatial offsets are detected, I09 used adaptive apertures (centred in the R image) to measure the bulk of the fluxes in the R and NB359 filters and derived the colour (i.e., the observed $f1500/f900$ ratios). The aperture diameters adopted vary from 2.0 to 4.0 arcsec, therefore, apart from the 'intrinsic' confusion due to the seeing, the relatively large apertures may include even more contaminants. Considering the sub-sample of 73 LBGs for which an offset has been measured, and adopting the median case of 1.0-arcsec radius and surface number density of galaxies with 26.5 $< U <$ 27.5 of 157 600 deg^{-2}, it turns out that there is 53 (2) per cent chance that at least three (seven) estimated colours are contaminated. With 1.5-arcsec radius, the chance is 96 (44) per cent. I09 suggested that the spatial offset may be related to the intrinsic nature and/or the geometry of the escape radiation process, maintaining however open the possibility of a superposition for part of the sample.

Finally, it is worth noting that the two LyC detected galaxies by S06 (SSA22a-D3 and SSA22a-C49) have been observed also by I09. In the case of SSA22a-D3, I09 noticed that the object is not visible in their NB359 image, even though the flux density limit is well below (two times) the limit reported by S06. The other source, SSA22a-C49, shows a NB359 signal (2.95σ level) spatially shifted with respect to the R band. From the ACS/F814 imaging (shown in I09, fig. 2, top right-hand panel), it is apparent that a distinct substructure within 1.0 arcsec from the brighter LBG, spatially consistent with the emission in the NB359 image. It would be important to obtain the redshift of such companion.

All these considerations suggest that the situation is still unclear and even though the pure foreground contamination may not entirely explain the direct LyC detections at high redshift, its effect is not negligible.

2.3 The integrated contribution of foreground sources

In the case of the stacking of LyC non-detections, the foreground contamination may play a role in the result. The stacking process increases the signal-to-noise ratio of the possible true emission of LyC, but at the same time a bias by foreground faint sources (not detected singularly) may arise. We calculate the expected average integrated contribution of the foreground blue sources in different rectangular apertures performing Monte Carlo simulations. In order to avoid possible contribution of the error fluctuation of the background, a noiseless image has been generated. It has been obtained by running the SExtractor algorithm (Bertin & Arnouts 1996) allowing the detection down to U-mag $\simeq$ 28.5 and requiring the 'OBJECT' output image (CHECKIMAGE_TYPE = OBJECT), that contains the detected sources separated by pixels with null values. 10 000 rectangular apertures have been randomly distributed over the noiseless and the original ultradeep VIMOS U-band images. On one side, the rectangle width (W) mimic the slit width and on the other side, the rectangle length (L, spatial direction) represents the inability to discriminate foreground sources closer than the seeing ($L = 2 \times$ seeing). S06 and Steidel et al. (2001) reported a typical seeing of $\gtrsim$ 0.8 arcsec, and used a slit width of 1.2 and 1.4 arcsec, respectively. Considering these values, the simulations have been performed adopting rectangular sizes ($W \times L$) of 1.2 $\times$ 1.6 and 1.4 $\times$ 1.6 arcsec^2. Since in the real case, relatively bright neighbours are easily recognized as contaminants, we have excluded from the possible interception the sources brighter than a given U-mag $U_{\rm max}$ (with $U_{\rm max} = 24$, 25 and 26). In this respect, it is important to check which effect has this cut in the optical magnitude domain, i.e. how many relatively bright sources in the optical are

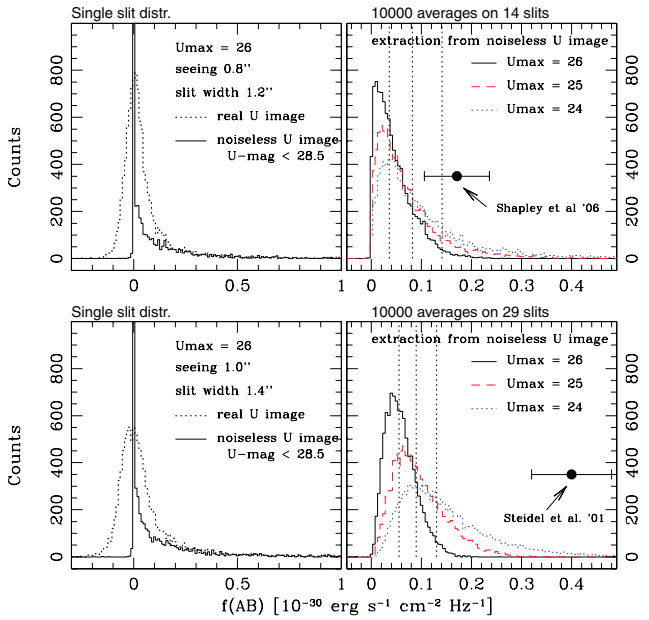

Figure 2. Upper panels: simulations on the LyC contamination in the case of S06. In the left-hand side the flux distribution of the 10 000 rectangular apertures randomly positioned over the observed U-band image (dotted line) and the noiseless image (with number counts down to ∼28.5, solid line) are shown. As expected, the noiseless image is peaked at the null flux value (corresponding to rectangular apertures not intercepting sources). In both the cases, the asymmetry towards brighter fluxes is the signature of pollution by interlopers (the case with $U_{\rm max} = 26$ is shown). In the right-hand panel, the distributions of the averages of over 14 rectangular apertures drawn from the noiseless image are shown, in the case of $U_{\rm max} = 24$, 25 and 26 (dotted, dashed and solid lines, respectively). The vertical dotted lines from left to right mark the median, the 1σ and 2σ confidence levels in the case $U_{\rm max} = 26$. The estimation reported by S06 (average of 14 spectra) is also shown with a filled circle. Lower panels: same as upper panels, but the simulations have been computed for the case of Steidel et al. (2001).

faint in the U band, and therefore recognizable as potential contaminants in the reference band (e.g. R). The mean R magnitudes of the LBG samples of S06 and Steidel et al. (2001) are 23.92 ± 0.32 and 24.33 ± 0.38, respectively. Using the ultradeep VLT/VIMOS, R-band catalogue of Nonino et al. (2009) that reaches R-mag $\simeq 29$ at 1σ within the 1-arcsec radius aperture, it turns out that with U-mag > 24 (i.e. $U_{\rm max} = 24$) the fraction of galaxies with R-mag < 24 (25) is 7 per cent (21 per cent). In the case of $U_{\rm max} = 25$ and 26, the fractions are 3 per cent (13 per cent) and 1 per cent (5 per cent) with R-mag < 24 (25), respectively. Therefore, in the following we refer to the last two cases, and in particular to the case with $U_{\rm max} = 26$ when calculating the quantities related to the LyC contamination.

The panels in the left-hand side of Fig. 2 show the flux (AB) distributions of the 10 000 random positioned rectangular apertures. The median and the dispersion of these distributions quantify the contamination to the LyC estimation for the single observation, the dotted line shows the distribution derived from the original U-band image and the solid line is that of the noiseless image. The difference between the two is clearly visible around the zero flux value, where in the case of the noiseless image there is a sharp peak, while in the real image case the peaked is around the zero value, but with a dispersion that is the contribution of fainter sources (U-mag > 28.5) and background noise fluctuation (see negative side of the distribution). More importantly, in both the cases, the asymmetry towards brighter fluxes is the signature of pollution by intercepted sources (modulated by the $U_{\rm max} = 26$ in the case shown). In the following, we adopt the noiseless image for the estimation of the LyC contamination. In order to simulate the effect in the average process, 10 000 averages adopting the observational conditions of S06 (14 sources, $W = 1.2$ arcsec and seeing 0.8 arcsec) and Steidel et al. (2001) (29 sources, $W = 1.4$ arcsec and seeing 1.0 arcsec) have been performed. The right-hand side of Fig. 2 shows these distributions drawn from the noiseless image, adopting $U_{\rm max} = 26$, 25 and 24 (solid, dashed and dotted lines, respectively). The medians, the 1σ and 2σ percentiles are reported in Table 2. Adopting the number counts down to 28.5, in the Steidel et al. (2001) configuration ($W \times L = 1.4 \times 2.0$ arcsec^2) and considering those realizations with $U_{\rm max} = 26$, the median, the 1σ and 2σ lower bounds of the distribution of the averages are 29.56, 29.03 and 28.62, respectively [they are (29.07, 28.48, 28.03) adopting $U_{\rm max} = 25$]. Similarly, in the S06 conditions ($W \times L = 1.2 \times 1.6$ arcsec^2) and considering those realizations with $U_{\rm max} = 26$, the median, the 1σ and 2σ lower bounds are 30.02, 29.13 and 28.54, respectively [they are (29.62, 28.72, 27.92) adopting $U_{\rm max} = 25$; see Fig. 2, right-hand panels, and Table 2 for a summary].

Table 2. Medians and 1σ, 2σ estimations of the integrated flux due to foreground sources for the samples of S06 (14 galaxies) and Steidel et al. 2001 (29 galaxies). The values have been derived from the noiseless images with number counts down to 28.5, 29.5 and 30.5. The latter has been built by extrapolating the observed number counts (see text for details).

Noiseless	$N = 14$			$N = 29$		
image	Median	1σ	2σ	Median	1σ	2σ
$U_{\rm max} = 25$						
$U \leq 28.5$	29.62	28.72	27.92	29.07	28.48	28.03
$U \leq 29.5$	29.25	28.54	27.83	28.74	28.29	27.90
$U \leq 30.5$	29.13	28.49	27.80	28.63	28.21	27.85
$U_{\rm max} = 26$						
$U \leq 28.5$	30.02	29.13	28.54	29.56	29.03	28.62
$U \leq 29.5$	29.53	28.89	28.40	29.08	28.71	28.39
$U \leq 30.5$	29.38	28.81	28.35	28.95	28.61	28.31

It is interesting to explore how these distributions change if the number counts are extrapolated down to fainter flux limits (U-mag = 30.5). This has been done by fitting a straight line to the observed counts between U-mag 25 and 28 with a slope of 0.2 in the (log(N) versus U-mag) plane (Table 1 shows the extrapolated values). From the real U-band image ('OBJECT' output image provided by SExtractor), 30 templates sources with U-mag $\simeq$ 27 have been extracted. Starting from this sample, the magnitude range 28.5 < U-mag < 30.5 has been populated by inserting randomly the galaxies appropriately dimmed according to the expected (extrapolated) number counts.

The resulting medians, 1σ and 2σ of the distributions down to these new magnitude limits are reported in Table 2. Increasing the U-mag limit for the number counts, it is apparent that the median values change more significantly than the dispersions (σ) and it is due to the fact that the probability to intercept (faint) sources increases significantly (the probability to intercept a contaminating source is $\gtrsim$20 per cent). Conversely, the variation of the scatter (σ) is lower, since it is mainly sensitive to the brighter contaminants, as expected when an average is computed. It is also worth noting that passing from U-mag 28.5, 29.5 and 30.5, the relative variations of the medians and the dispersions decrease, suggesting that

a further extrapolation (e.g. down to U-mag 31.5) does not change significantly the present results.

It is now possible to compare the observed residual flux reported in literature with the present simulations. Steidel et al. (2001) measured a residual flux in their composite spectrum of 29 LBGs of $m_{\rm AB} \simeq 27.4$ (AB) [$f900({\rm AB}) = 4.02 \times 10^{-31}$ erg s^{-1} cm^{-2} Hz^{-1}) and no direct detection was identified. They reported an observed ratio $(f1500/f900)_{\rm OBS}$ of 17.7 ± 3.8 that corresponds to a contrast of 3.1 mag in the AB scale. S06 using a slit width of 1.2 arcsec and the average over the 14 sources measured 28.33 (AB) also shown in the Fig. 2 (adopting their observed ratio $f1500/f900 = 58$ and the average magnitude of the sample $R = 23.92$). Considering the simulation with the noiseless image and number counts down to U-mag = 28.5, it turns out that the LyC estimations by Steidel et al. (2001) and S06 are significant at $>2\sigma$ level from the expected median foreground contamination. Adopting the resulting median flux values derived from the simulations, it is now possible to correct the LyC value observed by S06. Assuming the case of the noiseless image with number counts down to 30.5 and $U_{\rm max} = 25$ and 26, it turns out that the corrected residual $f900$ flux would be $\sim$1.9 (29.04 AB) and 1.6 (28.85 AB) times smaller than the value observed (28.33 AB), respectively. In the case of Steidel et al. (2001), the average residual $f900$ flux (magnitude 27.4) is brighter than S06, so the correction is less important. The corrected residual $f900$ flux would be $\sim$1.5 (27.82 AB) and 1.3 (27.70 AB) times smaller, adopting the medians calculated from the noiseless images down to U-mag 30.5 with $U_{\rm max} = 25$ and 26, respectively. This would also decrease the average relative escape fraction ($\langle f_{\rm esc,rel} \rangle$) by the same factors.[2]

A way to further investigate the contamination occurrence due to foreground blue sources on $z \sim 3$–4 galaxies is to use high-resolution, deep and multicolour images as those obtained from the GOODS project. This is the argument of the next section.

3 *U*-BAND DETECTED LBGS AT $z > 3.48$ IN THE GOODS-S

An observational test can be performed directly on the GOODS-S area by cross-correlating the VLT/VIMOS U-band catalogue with the list of available B-band dropout galaxies observed during the VLT/FORS2 campaign with known spectroscopic redshift (Vanzella et al. 2008, 2009) and for which the Lyman limit is redder than the filter transmission. The astrometric solution between the U and the ACS catalogues gives an rms in RA and Dec. lower than 0.1 arcsec on average (Nonino et al. 2009). Adopting radius of 0.5, 1.0 and 1.3 arcsec in the matching, it turns out that one, four and 11 galaxies out of 36 with redshift between 3.47 and 4.3 have an U-band detection with U-mag in the range 26.1–29.4.[3] Therefore, the numbers we obtain matching the U-band and the ACS catalogue are fully consistent with the random occurrence of foreground superpositions (see Table 3).

In the following, we consider the matching within 1 arcsec (since typically ground-based imaging is performed with seeing better than 1 arcsec). In this case, the four LBGs that lie within 1.0 arcsec are (1) GDS J033225.16−274852.6 ($U = 26.57$), (2) GDS J033220.97−275022.3 ($U = 27.17$), (3) GDS J033226.28−275245.7 ($U = 28.47$) and (4) GDS J033236.83−274558.0 ($U = 28.63$) (see Fig. 3). The magnitudes of the involved U-band detected sources range within $26.57 < U < 28.63$, corresponding to a percentage of the observed continuum flux of the LBGs in the i_{775} band ($\sim$1600–1700 Å rest frame) of 2–10 per cent, a quantity that resembles the observed LyC values often reported in literature. Apart from the brighter case (1) in which the contamination comes from the relatively bright galaxy close to the LBG (GDS J033225.09−274852.6, $z_{850} = 22.61$, $B_{435} = 26.0$), in the other three cases the depth of the GOODS (and *HUDF*) area allows to visually appreciate the presence of at least one compact blue source (not distinguishable in the ground-based R band) shifted with respect to the targeted LBG and within 1-arcsec distance. In particular, in the case (4), the fainter in the U band among the four discussed, the spatial offset is $<$0.5 arcsec, and sits in the *HUDF*. In the next section, we report on this (extreme) system as an example of LyC contamination.

Table 3. Probabilities per cent $P(K)$ and $P(\geq K)$ that 'K' and 'at least K' galaxies out of 36 (N) in the GOODS-S field used to check the occurrence of foreground contamination within 0.5 and 1.0 arcsec are reported (assuming U-band number counts down magnitude 28.5). The number of cases observed (1/36 with 0.5-arcsec and 4/36 with 1.0-arcsec radius) is highlighted in bold face.

	$P(\geq K)$	$P(\geq K)$	$P(K)$	$P(K)$
K	0.5-arcsec radius	1.0-arcsec radius	0.5-arcsec radius	1.0-arcsec radius
0	100.0	100.0	31.6	0.8
1	**68.4**	99.2	**37.0**	4.1
2	31.4	95.2	21.1	10.2
3	10.4	84.9	7.8	16.8
4	2.6	**68.2**	2.1	**19.9**
5	0.5	48.2	0.4	18.4

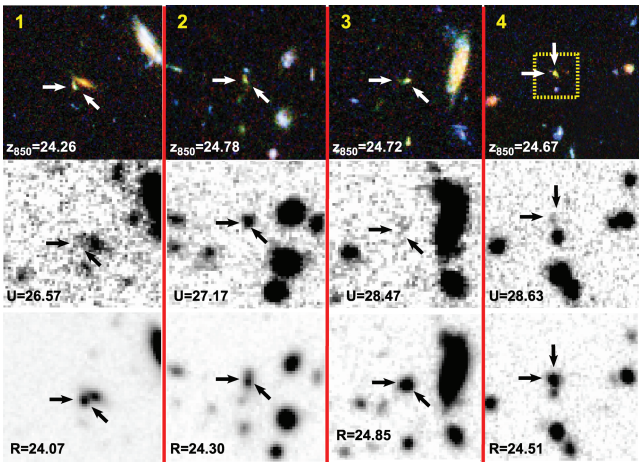

Figure 3. BVi composite ACS colour images (top), the VLT/VIMOS U-band images (middle) and the VLT/VIMOS R-band images (bottom) of the four cases (out of 36 LBGs) that satisfy the matching between the U-band and the ACS v2.0 catalogues, adopting a radius of 1.0 arcsec (the cut-outs of 10-arcsec size show several blue compact sources in the blank field). From left to right, the U-mag increases and the arrows indicate the position of the LBGs. The upper-right case is shown with more detail in Fig. 4 (dotted square).

[2] See Steidel et al. (2001) or S06 (equation 1) for the definition.

[3] At redshift larger than 3.4, the 912 Å limit is redder than the VIMOS U-band response (Nonino et al. 2009). It is also known that one of the four quadrants of the VIMOS U-band image shows a read leak at $\lambda \sim 4850$ Å. However dedicated simulations show that it has a negligible effect ($\simeq$0.1 per cent) (see Nonino et al. 2009, appendix C). Moreover the quadrant is not affecting the cases we are discussing here, especially that on the *HUDF*.

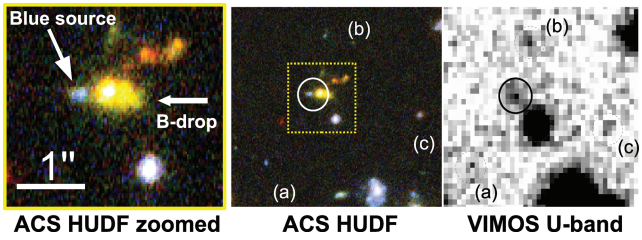

Figure 4. Left: detail of ACS *HUDF* colour image of the *B*-band dropout galaxy (case 4 in Fig. 3) at redshift 3.797. A blue compact source at ∼0.4 arcsec from the centre of the LBG is indicated, superimposed to the high-redshift galaxy. Middle: 10 arcsec side field around the LBG. The yellow dotted square is shown in the left-hand panel. Other three compact *U*-detected sources are marked (a), (b) and (c). Right: the VLT/VIMOS *U*-band image of the middle panel (Nonino et al. 2009). The detection at the position of the high-redshift galaxy is clear (5σ, solid circle), in which the presence of a non-resolved (in the *U* band) blue compact source is evident in the *HUDF* image (left-hand side).

3.1 An exemplary faint foreground contamination at $z = 3.797$ in the *HUDF*

An example of *false* detection of escape radiation of one of the *B*-band dropout galaxies discussed above is shown in the right-hand panel of Fig. 4. The clear detection in the *U* band is shown (*U*-mag 28.63 ± 0.2) at the position of the galaxy GDS J033236.83−274558.0 at redshift 3.797. In the left-hand panel of the same figure, the colour image extracted from the *HUDF* is shown. It is clearly visible a blue compact source superimposed on the $z = 3.797$ galaxy slightly offset by $\lesssim$0.4 arcsec (this blue source is visible also in the ACS/B435 and V606 bands). We note that the LBG and the blue source have been detected as a single galaxy in the *HUDF* catalogue by Coe et al. (2006). If the blue spot is not a contaminant, then it would be an ultradeep, high-resolution 'morphologically detected' LyC case at high redshift. It is not clear what would be the morphological appearance of galaxies showing LyC escape photons at $\lambda < 912$ Å , however, the system can be easily explained by the presence of a foreground source rather than a shifted 'hole' where Lyman photons can escape. Therefore we favour the simpler interpretation of a superposition case. It is worth noting that this system would appear as a single source if observed with lower spatial resolution, as in the *R* band or deep *U* image (seeing 0.8 arcsec, where presumably the blue source is entirely contributing to the *U*-band detection). A deep spectroscopic or narrow-band observation of this system with a seeing larger than 0.5 arcsec would detect a signal below 912 Å erroneously ascribed to the source at higher redshift. In particular, given the *U*-mag of 28.63 and $i_{775} = 24.67$ the polluting source mimic an observed $(f1500/f900)_{\rm OBS} \sim 38$. This value is at least three times larger than the current LyC detections (S06 and I09), and comparable to the reported estimates of stacked spectra, i.e. 17.7 and 58 reported by Steidel et al. (2001) and S06, respectively.

4 CONCLUDING REMARKS

Depending on the seeing conditions and/or the aperture sizes adopted to carry out the photometry/spectroscopy, the contamination probability by foreground blue sources on the estimation of the ionizing radiation may not be negligible. In particular in the cases reported by S06 and I09, it turns out that the probability of foreground contamination for at least half of the direct LyC detections is ∼30 and 50 per cent, respectively. Among the direct LyC detections in I09, there are cases of spatially offset emission (in the case of LBGs) and cases of extremely high escape fraction (even larger than unity). We argue that, other than a possible complex physical explanation (e.g. Inoue 2010), these suspicious systems should better be investigated with higher resolution and multiband imaging, since they are statistically compatible with superposition effects.

Also in the case of statistical LyC detection, the foreground contamination plays a role in the global result. A stacking process increases the signal-to-noise ratio of the possible true LyC emission, but at the same time a bias by foreground faint sources (not detected individually) may arise. The issue has been addressed by computing Monte Carlo simulations from which, taking advantage of the ultradeep VLT/VIMOS *U*-band number counts (Nonino et al. 2009), we calculated the median contribution of foreground sources to the residual flux measure below the Lyman limit. From these calculations, it turns out that the current estimations of LyC emission from stacked spectra at redshift ∼3 are beyond 2σ from the expected median foreground contribution.

The simple foreground contamination may not entirely explain the cases of direct escape fraction observed or the limits derived from the stacking, nevertheless the calculations and the examples reported here demonstrate the need for caution in LyC measurements at high redshift. This systematic error has to be considered when attempting to measure the LyC escape fraction and its evolution with redshift and the contribution of galaxies to the UV background. For example, from simulations it turns out that the corrected observed $f900$ flux reported by S06 would be ∼1.6–1.9 times smaller than the reported value. Differently, the correction for the Steidel et al. (2001) estimation is less effective (a factor of ∼1.3), since their residual flux is ∼1 mag brighter than S06. Consequently the relative escape fractions are dimmed by the same factors. It is worth noting that in stacked images of tens and hundreds of galaxies at redshift ∼1, there is currently no direct detection (Malkan et al. 2003; Siana et al. 2007, 2010; Cowie et al. 2009). On the one hand, it may reflect indirectly the redshift distribution of the (faint *U*-mag > 26) blue compact sources that populate the ultradeep *U*-band image. Since no evident contaminations have been currently measured at redshift ∼1, the bulk of the (faint) blue compact sources would be at redshift >1. On the other hand, being these objects *U*-band detected, their typical redshift is most probably smaller than 3 (i.e. they are not *U*-band dropouts). For the brighter part of the distribution (*U*-mag < 26.5), a further constraint on the redshift comes from the MUltiwavelength Southern Infrared Catalog (MUSIC) photometric redshift catalogue (Grazian et al. 2006), from which they span the interval $0 < z < 3$.

Conversely, in the case of LyC observations at $z > 3$ the contribution of such blue galaxies as contaminants largely increases. In general, the fraction of galaxies contaminated ranges between ∼3 and ∼15 per cent, varying from seeing 0.5 to 1.0 arcsec, respectively, and assuming number counts down to *U*-mag ∼ 28.5. On the one hand simulations predict an evolution (increase) of the escape fraction with increasing redshift (e.g. Razoumov & Sommer-Larsen 2007), on the other hand also the contamination by foreground sources it is expected to increase, with a more significant effect for fainter LBGs ($R > 24$). Therefore, if the contamination is not taken into account properly, the observational constraints on the evolution of the escape fraction may be biased, particularly at faint limits where the population of blue compact sources increases in number density. In order to produce a robust LyC measurements at

$z \gtrsim 3$ high spatial resolution, multiband and ultradeep imaging are necessary to exclude the spurious cases.

ACKNOWLEDGMENTS

We would like to thank the referee (I. Iwata) for very constructive comments and suggestions. EV would like to thank M. Giavalisco for useful comments and discussions about this work. We are grateful to the ESO staff in Paranal and Garching who greatly helped in the development of this programme. EV acknowledges financial support from contract ASI/COFIN I/016/07/0 and PRIN INAF 2007, 'A Deep VLT and LBT view of the Early Universe'.

REFERENCES

Beckwith S. V. W. et al., 2006, AJ, 132, 1729
Bertin E., Arnouts S., 1996, A&A, 117, 393
Coe D., Benítez N., Sánchez S. F., Jee M., Bouwens R., Ford H., 2006, AJ, 132, 926
Cowie L. L., Barger A. J., Trouille L., 2009, ApJ, 692, 1476
Faucher-Giguère C.-A., Lidz A., Hernquist L., Zaldarriaga M., 2008, ApJ, 688, 85
Giallongo E., Cristiani S., D'Odorico S., Fontana A., 2002, ApJ, 568, 9
Gnedin N. Y., Kravtsov A. V., Chen H., 2008, ApJ, 672, 765
Grazian A. et al., 2006, A&A, 449, 951
Inoue A. K., 2010, MNRAS, 401, 1325
Iwata I. et al., 2009, ApJ, 692, 1287 (I09)
Malkan M., Webb W., Konopacky Q., 2003, ApJ, 598, 878
Nonino M. et al., 2009, ApJS, 183, 244
Razoumov A. O., Sommer-Larsen J., 2007, ApJ, 668, 674
Razoumov A. O., Sommer-Larsen J., 2010, ApJ, 710, 1239
Shapley A. E., Steidel C. C., Pettini M., Adelberger K. L., Erb D. K., 2006, ApJ, 651, 688 (S06)
Siana B. et al., 2007, ApJ, 668, 62
Siana B. et al., 2010, ApJ, in press (arXiv:1001.3412)
Steidel C. C., Pettini M., Adelberger K. L., 2001, ApJ, 546, 665
Vanzella E. et al., 2008, A&A, 478, 83
Vanzella E. et al., 2009, ApJ, 695, 1163
Yajima H., Umemura M., Mori M., Nakamoto T., 2009, MNRAS, 398, 715

This paper has been typeset from a TEX/LATEX file prepared by the author.